Plectin promotes melanoma tumor formation by regulation of Rous sarcoma oncogene activity

Kana Mizuta
Kyushu Dental University
Takuma Matsubara (r15matsubara@fa.kyu-dent.ac.jp)
Kyushu Dental University
Akino Goto
Kyushu Dental University
William N. Addison
Kyushu Dental University
Mitsushiro Nakatomi
University of Occupational and Environmental Health
Kou Matsuo
Kyushu Dental University
Yukiyo Tada-Shigeyama
Kyushu Dental University
Hiromi Honda
Kyushu Dental University
Izumi Yoshioka
Kyushu Dental University
Shoichiro Kokabu
Kyushu Dental University

Research Article

Keywords: Melanoma, Src, Plectin, tumor genesis, cell adhesion

Posted Date: April 1st, 2022

DOI: https://doi.org/10.21203/rs.3.rs-885454/v2

Abstract

Background

Melanoma is a malignant tumor that is characterized by high proliferation and aggressive metastasis. To address the efficient treatment of melanoma, the molecular mechanisms of the proto-oncogene, Rous sarcoma oncogene (Src), which is highly activated and promotes cell proliferation, migration, adhesion, and metastasis in melanoma, should be understood. Plectin has recently been identified as an Src-binding protein that regulates Src activity in osteoclasts. Plectin, a cytoskeleton-regulatory protein, is a candidate biomarker of certain tumors because of its high expression and the target of anti-tumor reagents such as ruthenium pyridinecarbothioamide, although the molecular mechanisms by which plectin works in melanoma are still unclear. In this study, we examined its pathological role in melanoma tumor formation.

Methods

We established plectin knock-out B16 cells, the mouse melanoma cell line, with CRISPR/Cas9 system. The expression of plectin and activity of Src were examined by western blotting analysis. The tumors were formed at 2 weeks after subcutaneous injection of B16 cells in nude mice and analyzed by Hematoxylin-Eosin (H-E) staining. Cell proliferation was evaluated by cell counting kit-8, expression of cyclin D1 and Ki-67. Cell aggregation and adhesion were assessed by spheroid formation and cell adhesion assay.

Results

Depletion of plectin induced low-density and sparce tumor formation by melanoma cells in vivo. In vitro experiments revealed that plectin-deficient melanomas exhibit reduced cell proliferation and suppressed cell-to-cell adhesion. Because Src activity is reduced in plectin-deficient melanomas, we examined the relationship between plectin and Src signaling. Src overexpression restored Src activity and rescued cell proliferation and cell-to-cell adhesion in plectin-deficient melanomas.

Conclusion: These results suggest that plectin is required for tumor formation by promoting cell proliferation and cell-to-cell adhesion through Src signaling activity in melanoma cells.

Background

Melanoma is an aggressive tumor derived from skin melanocytes [1, 2]. Patient prognosis is usually poor because the rapidly proliferating melanoma progresses from radial to vertical growth and metastasizes frequently [1, 2]. Recently developed therapeutic interventions target melanoma metastasis by blocking immune checkpoints using cytotoxic T-lymphocyte-associated antigen 4 (CTLA-4) or programmed death 1 (PD-1) inhibitors [3]. However, these reagents occasionally cause adverse immune-related events such as large intestinal inflammation, interstitial pneumonia, and type I diabetes [4]. Furthermore, the failure of

some tumors to respond to therapy and acquired resistance during immune checkpoint therapy can occur. In addition, melanoma secretes immune suppressing agents such as cortisol and lymphotoxic intermediates [5]. Therefore, novel approaches need to be developed.

Rous sarcoma oncogene (Src), a non-receptor tyrosine kinase, plays a physiological role in several cellular processes [6–9] including proliferation, adhesion, migration, and actin filament organization [7, 8]. Src signal transduction is initiated by the phosphorylation of substrates such as protein tyrosine kinase 2 beta (Pyk2) [8, 10] or actin-binding proteins. Src activation suppresses stress fiber formation, leading to the conversion of spindle-shaped cells into round cells with dot-like actin structures [11]. In pathological conditions, Src, which was originally identified as the first proto-oncogene, is related to malignancy, growth, and invasion of several tumors, including melanoma [12–17].

Plectin is a large protein consisting of more than 4000 amino acids. Plectin binds to actin, microtubules, and intermediate filaments, and regulates the cytoskeleton, cell shape, and chromosomal structure [18, 19]. Previously, it was demonstrated that plectin is essential for Src activation during osteoclastogenesis. In osteoclasts, plectin acts as a scaffold for the recruitment of Src and Pyk2 [20] substrates. Plectin is a candidate biomarker for certain types of tumors because its expression in tumor specimens is higher than that in surrounding normal tissues [21–23]. Recently, a novel anti-tumor agent targeting plectin, ruthenium pyridinecarbothioamide, was shown to suppress tumor growth in a B16 melanoma cell model [24, 25]. These studies suggest that plectin plays an important role in melanoma pathology and is a good candidate for novel melanoma therapies. However, the exact mechanism through which plectin regulates melanoma remains unknown.

In this study, we examined the role of plectin and its interaction with Src signaling in melanoma cell behavior.

Methods

Cell culture

B16 (RRID: CVCL_F936) and HMV-II (RRID: CVCL_1282) cells were purchased from RIKEN BRC (Ibaraki, Japan) on 2 October 2018. B16 cells were maintained in Dulbecco's Modified Eagle Medium (DMEM; Fujifilm Wako, Osaka, Japan) supplemented with 10% fetal bovine serum (fetal bovine serum [FBS]; Nichirei – lot number S.18M00C) [26]. HMVII cells were maintained in Ham's F12 medium (Fujifilm Wako), supplemented with 10% FBS. HMV-II cells were authenticated by STR (or SNP) profiling using RIKEN BRC. B16 and HMV-II cells were cultured and used to perform experiments in mycoplasma-free conditions. Cells were transfected using Lipofectamine 2000 (Thermo Fisher Scientific, Waltham, MA, USA), according to the manufacturer's instructions.

Establishment of plectin knockout B16 cells and knockdown of plectin in HMVII cells

Mouse plectin-targeting oligonucleotide 5’- GGCGATGTCGGAGATAGTCC -3’ was cloned into a pGuide-it-ZsGreen1 vector (Takara Bio Inc., Shiga, Japan) and transfected into B16. Single-cell clones were selected using limiting dilution. Plectin expression was determined using western blot analysis [20, 27] .

Human plectin targeting oligonucleotides
5’- GGCGTAGGAAATACAGTTGTGATCTCGAGATCACAACTGTATTTCCTACGTTTTT -3’ (human plectin shRNA1) and 5’- GGCCTCTTCGATGAGGAGATGAACTCGAGTTCATCTCCTCATCGAAGAGGTTTTT -3’ (human plectin shRNA2) were cloned into pSIREN-Retro-Q-Zsgreen (Takara Bio Inc.), as described previously [20, 27].

The Src plasmid (#13658) was purchased from Addgene (Cambridge, MA, USA) and subcloned into a pcDNA 3.1 (-) plasmid (Thermo Fisher Scientific) with a Flag-tag using PCR [28, 29].

Western blot analysis

Cells were lysed with a 1% Triton X-containing lysis buffer, as described previously [20]. Lysates were boiled with sodium dodecyl sulfate (SDS) sample buffer for 5 min at 95 °C [20]. Samples were separated on 7.5%, 10%, and 12% SDS-PAGE gels and transferred to polyvinylidene difluoride (PVDF) membranes. After blocking with 5% bovine serum albumin (BSA), the membranes were incubated with primary antibodies. The antibodies used were anti-Plectin-1 (#12254), anti-Src pY416 (#2101), anti-Pyk2 (#3292), anti-Pyk2 pY402 (#3291) (Cell Signaling Technology, CST, Danvers, MA), anti-Src (ab-1) (Merck, Darmstadt, Germany), anti-DDDDK-tag (Fla-1), anti-GAPDH mAb-horseradish peroxidase-conjugated (HRP)-DirecT (Medical & Biological Laboratories, MBL, Tokyo, Japan), and β-actin (A2228) (Sigma Aldrich Chemicals, St. Louis, MO). The membranes were then incubated with HRP-conjugated anti-mouse or anti-rabbit secondary antibodies. Finally, the blots were imaged using a LAS4000 (Fujifilm Wako) with Immobilon ECL Ultra Western HRP Substrate (Merck).

Immunocytochemical analysis

A total of 1×10^4 cells were plated on a cover glass and cultured for 1 d. Cells were fixed with 3.7% formaldehyde and washed with phosphate buffered saline (PBS). Cells were permeabilized with PBS containing 0.2% Triton X100 and blocked with 5% BSA for 2 h or 4 h. Cells were then incubated with anti-Ki-67 rabbit monoclonal antibody (ab92742, Abcam Cambridge, UK) and anti-DDDDK-tag in 5% BSA at 4 °C overnight. Target proteins were visualized using Alexa 488-conjugated or Alexa 555-conjugated secondary antibodies (Thermo Fisher Scientific). The actin cytoskeleton was visualized using rhodamine phalloidin (Thermo Fisher Scientific). Nuclei were visualized using 4',6-diamidino-2-phenylindole (DAPI). Slides were imaged using a BZ-X810 microscope (Keyence, Osaka, Japan) and analyzed using ImageJ software (NIH).

Animals and tumor injection

Ten-week-old male BALB/cAJcl-nu/nu mice were purchased from CLEA Japan, Inc. (Tokyo, Japan). All mice were used in accordance with the guidelines of the Animal Care and Use Committee of Kyushu Dental University, based on the Animal Research: Reporting of *In Vivo* Experiments (ARRIVE) guidelines. This study was approved by the Animal Care and Use Committee of Kyushu Dental University (Approval #19-020). The mice were housed under specific pathogen-free conditions. Anesthesia was performed by intraperitoneal injection of an anesthetic agent cocktail (0.3 mg/kg body weight (b.w.) medetomidine, 4.0 mg/kg b.w. midazolam, and 5.0 mg/kg b.w. butorphanol) [30]. Anesthetized mice were injected subcutaneously with 1×10^5 cells in a 100 µL volume [26] After 2 weeks, mice were anesthetized with an anesthetic agent cocktail and perfused by injecting 4% paraformaldehyde in PBS from cardiac apex [31]. Tumors were then dissected, measured with calipers, and weighed using an electronic balance scale. Volumes were calculated using the formula $\text{width}^2 \times \text{length} \times 0.52$, as previously described [32, 33]. Sections of 10 µm were prepared using a cryostat. The sections were stained with hematoxylin and eosin (H&E) and imaged using a BZ-X810 microscope. The space between cells was measured using ImageJ software.

Cell proliferation assay

The cells were plated at a density of 5,000 cells/well in 96-well plates. Cell viability was assessed every 24 h using the Cell Counting Kit-8 (Dojindo, Kumamoto, Japan), according to the manufacturer's protocol [26].

Reverse transcription and quantitative PCR (qPCR)

Total RNA was isolated using the FastGene™ RNA Basic Kit (Nippon Genetics, Tokyo, Japan) and reverse-transcribed into cDNA using the High-Capacity cDNA Reverse Transcription Kit (Thermo Fisher Scientific) [34]. Real time quantitative (q)PCR was performed using a Quantstudio 3 system (Thermo Fisher Scientific) with specific primers for murine Cyclin D1 (*Ccnd1*); (forward, 5'- tttctttccagagtcatcaagtgt -3'; 5'- tgactccagaagggcttcaa -3'), human Cyclin D1 (*CCND1*); (forward, 5'- tctacaccgacaactccatccg -3'; 5'- tctggcattttggagaggaagtg -3'), human PLECTIN (*PLEC*); (forward, 5'- agcgtgagaaggagaagctcca -3'; 5'- cagagaggaagctttgctgcag -3'), murine β-actin (*Actb*); (forward, 5'- aaggccaaccgtgaaaagat -3'; reverse, 5'- gtggtacgaccagaggcatac -3'), and human β-actin (*ACTB*); (forward, 5'- caccattggcaatgagcggttc -3'; reverse, 5'- aggtctttgcggatgtccacgt -3') [35, 36]. Gene expression levels were calculated using the ΔΔCT method and normalized to that of β-actin.

Spheroid formation

Cells were seeded at a density of 5,000 cells in 15 µL of media on the inner side of a dish lid. The lid was placed upside down on a PBS-filled plate Cells were cultured for 7 d at 37 °C, with 5% CO. Images of spheroids were taken with a Leica EZ4 HD microscope (Leica, Germany) and analyzed using ImageJ software. The volumes were calculated using the formula width2 × length × 0.52, similar to that used for the tumor.

Cell adhesion assay

Fibronectin (10 µg/mL) was coated in 96-well plates by overnight incubation at 4 °C. Wells were then blocked with 2% BSA for 2 h at room temperature (RT). Cells were plated at a density of 3×10^4 cells per well in serum-free medium and allowed to attach for 2 h at 37 °C with 5% CO. Non-adherent cells were washed away with serum-free medium. The remaining adherent cells were fixed using 1% glutaraldehyde/PBS for 10 min and stained with crystal violet in 2% methanol/PBS for 20 min at RT with shaking. Crystal violet was solubilized with 1% SDS and quantified by absorbance measurement at 595 nm using a microplate reader (Bio-Rad, Hercules, CA). Adherent cells were counted using ImageJ software.

Data analysis and statistics

The statistical significance of the differences between groups was analyzed using one-way ANOVA followed by a Tukey-Kramer post-hoc test. Statistical significance was set at $p < 0.05$. Data are expressed as mean ± standard deviation of the mean (n = number of samples). All experiments were independently performed at least twice and similar results were obtained.

Microarray data mining

Dataset GDS1375 from the NCBI Gene Expression Omnibus (GEO) was analyzed for plectin and Src gene expression in melanoma patient samples, as previously described [26, 37]. Means were compared using Kruskal-Wallis followed by Dunn's post hoc test.

Results

Src signaling is impaired in plectin-deficient melanoma cells

To examine the role of plectin in melanoma, two types of plectin-deficient murine B16 melanoma cells (PKO cells) and plectin shRNA-mediated knockdown human HMV-II cells were generated. The level of

phospho-Pyk2 (Tyr402), an indicator of Src signal activation, was decreased in both types of plectin-deficient cells (Figs 1A, 1B, and S1A) compared to that in control cells. Moreover, the binding of Src to Pyk2 was reduced in PKO cells (Fig 1C). Plectin-deficient cells were spindle-shaped and less round than control cells (Figs 1D and S1B). Spindle-shaped cells with thick and long actin fibers are characteristic of disturbed Src signaling. Thus, the depletion of plectin impairs Src signaling in melanoma cells.

Plectin regulates cell proliferation and adhesion of melanoma

To determine the function of plectin in tumor formation in vivo, control or PKO cells were subcutaneously injected into the backs of nude mice (Fig 2A). There were no significant differences in tumor weight or volume between control and PKO cells (Figs S2A and S2B). However, the density of PKO tumors was lower than that of the control (Fig 2B). Histological analysis showed that the distance between cells within the PKO tumor was greater than that between the control tumor cells (Fig 2C). These data suggest that plectin may affect both the cell number and intercellular connections.

Next, the effects of plectin on the number of cells in vitro were examined. The number of viable cells significantly reduced after plectin depletion (Figs 3A and S3A). The mRNA levels of Cyclin D1, a regulator of cell cycle progression, were also decreased in plectin-deficient cells. The number of Ki-67 positive cells, a proliferation marker, was also decreased in plectin-deficient cells (Figs 3B, 3C, S3B and S3C), indicating that plectin regulates the proliferation of melanoma cells.

A spheroid formation and cell adhesion assays was performed to explore the role of plectin in intercellular cell connections. Similar to tumor formation in vivo, plectin-deficient cells formed larger spheroids than the control cells (Figs 4A and S4A). In addition, cell attachment was reduced in plectin-deficient cells compared to that in control cells in an adhesion assay (Figs 4B and S4B). This suggests that plectin plays an important role in both cell proliferation and cell-to-cell adhesion of melanoma cells.

Overexpression of Src rescues plectin knockout phenotype in melanoma

To determine whether plectin affected melanoma cell behavior through Src signaling, Src was overexpressed in PKO cells (Fig 5A). Overexpression of Src in PKO cells caused the cells to regain a rounded shape, with actin accumulation at the periphery of the cell (Fig 5B). Overexpression of Src rescued the decrease in the number of viable cells and Ki-67 positive cells. Src overexpression did not affect the viability of control cells (Figs 5C and 5D). Src overexpression in PKO cells led to the formation of small, tightly packed spheroids similar to control cells. Src overexpression also restored the adhesion ability of PKO cells to levels similar to those of control cells (Figs 5E and 5F).

Discussion

In this study, we demonstrated that plectin was essential for Src activation in melanoma cells. This is similar to our previous observations in osteoclasts [20]. In plectin-deficient melanomas, proliferation and adhesion are impaired. Overexpression of Src signaling partially rescued defective proliferation and adhesion. This suggests that plectin regulates the proliferation and adhesion of melanoma cells through Src-dependent and Src-independent mechanisms.

In tumor cell proliferation, Src mediates growth factor signaling by activating Ras GTPase and mitogen-activated protein kinases (MAPKs) [8]. Src and cyclin-dependent kinase 1 (Cdk1) have common substrates related to cell proliferation [38, 39]. Plectin is known to be involved in cell proliferation independently of Src. Cdk1 interacts with plectin and regulates the rearrangement of the cytoskeleton during interphase to promote mitosis [19]. Plectin directly binds and organizes actin, microtubules, and intermediate filament networks at each step of the cell cycle [19]. Therefore, cell division is disrupted in the absence of plectin. Src is a major regulator of cell adhesion and aggregation. Cadherin, a Src substrate, is important for cell-to-cell contact in desmosomes and tight junctions [40, 41]. Src signaling also promotes focal adhesion formation via Pyk2 and Rho GTPase activation [42–44]. Plectin plays an Src-independent role in cell adhesion and aggregation [45]. Plectin binds directly to keratin networks to form desmosomes [46, 47]. Therefore, plectin depletion leads to disruption of keratin networks in the skin and causes skin blistering or epidermolysis bullosa simplex [46, 48, 49].

Analysis of a GEO dataset showed that plectin-and Src-related genes are highly expressed in human primary melanoma in patients compared to human melanocytes (Fig S5). When considered with our experimental data, plectin may be required for malignancy and primary tumor formation in melanoma. During metastasis, plectin may play a positive role in the invasion and migration into the vascular system. Src signaling and plectin are essential for organizing actin structures in invadosomes [50, 51]. Plectin may also be necessary for cell anchoring to the target tissue during metastasis or separation of cells from the primary tumor mass. Therefore, the role of plectin in melanoma progression may differ at each step.

An anti-tumor agent targeting plectin, ruthenium pyridinecarbothioamide, has been recently developed for the treatment of melanoma [24, 25]. Our present study strongly supports a role for plectin in melanoma during early stage events, such as primary tumor formation. However, the effects of plectin inhibition during the late stage of melanoma remain unclear. Furthermore, data from the Human Protein Atlas (https://www.proteinatlas.org/ENSG00000178209-PLEC/pathology/melanoma) and The Cancer Genome Atlas (TCGA) showed that melanoma patients with high plectin expression survived significantly longer than those with low expression levels. This suggests that the suppression of plectin may promote melanoma after the formation of the primary tumor because the primary tumor had already been formed upon diagnosis. Further studies, especially on invasion and metastasis, are required to clarify the role of plectin in melanoma progression.

Conclusion

Plectin plays a key role in robust tumor formation in melanoma by regulating cell proliferation and aggregation through Src signaling.

Declarations

Author contributions

T. M. and S. K. designed the study. K. M. and T. M. performed the experiments. A.G. and M.N. analyzed tumor tissue. K. M. T. M., S. K. wrote the first draft. W. A. provided feedback. M.K., Y.T-S., T. Y., J. N., H.H., I. Y. and S. K. performed literature review.

Competing interests

The authors declare that they have no competing interests.

Funding

This work was supported by grants from the Japan Society for the Promotion of Science (KAKENHI 18K09509 and 21K09830 to T. M., 21K10078 to Y.T-S., 21K10260 to H.H., 20K09924 to K.M., 20K10185 to I. Y., and 21H03144 to S.K.). This work was also supported by R1 Fukuoka Foundation for Sound Health Cancer Research Fund to W. A.

Acknowledgement

We would like to thank Editage (www.editage.com) for English language editing. We thank Prof. Kentaro Ono (Kyushu Dental University) for advice on statical analysis.

Availability of data and materials

The datasets used and/or analyzed during the current study are available from the corresponding author on reasonable request. The dataset in Fig. S5 is available from GSE1375 dataset of NCBI Gene Expression Omnibus (GEO).

References

1. Rigel DS, Carucci JA. Malignant melanoma: prevention, early detection, and treatment in the 21st century. CA Cancer J Clin. 2000;50:215–36; quiz 237–40.

2. Perera E, Gnaneswaran N, Jennens R, Sinclair R. Malignant Melanoma. Healthcare (Basel). 2013;2:1–19.

3. Larkin J, Hodi FS, Wolchok JD. Combined nivolumab and ipilimumab or monotherapy in untreated melanoma. The New England journal of medicine. 2015;373:1270–1.

4. Horvat TZ, Adel NG, Dang T-O, Momtaz P, Postow MA, Callahan MK, et al. Immune-related adverse events, need for systemic immunosuppression, and effects on survival and time to treatment failure in patients with melanoma treated with ipilimumab at memorial Sloan Kettering cancer center. J Clin Oncol. 2015;33:3193–8.

5. Slominski AT, Carlson JA. Melanoma Resistance: A Bright Future for Academicians and a Challenge for Patient Advocates. Mayo Clin Proc. 2014;89:429–33.

6. Soriano P, Montgomery C, Geske R, Bradley A. Targeted disruption of the c-src proto-oncogene leads to osteopetrosis in mice. Cell. 1991;64:693–702.

7. Vara JÁF, Cáceres MAD, Silva A, Martín-Pérez J. Src family kinases are required for prolactin induction of cell proliferation. Mol Biol Cell. 2001;12:2171–83.

8. Kim LC, Song L, Haura EB. Src kinases as therapeutic targets for cancer. Nat Rev Clin Oncol. 2009;6:587–95.

9. Okada M. Regulation of the SRC family kinases by Csk. Int J Biol Sci. 2012;8:1385–97.

10. Zhao M, Finlay D, Zharkikh I, Vuori K. Novel role of Src in priming Pyk2 phosphorylation. PLoS One. 2016;11:e0149231.

11. Berdeaux RL, Díaz B, Kim L, Martin GS. Active Rho is localized to podosomes induced by oncogenic Src and is required for their assembly and function. J Cell Biol. 2004;166:317–23.

12. Irby RB, Yeatman TJ. Role of Src expression and activation in human cancer. Oncogene. 2000;19:5636–42.

13. Qi J, Wang J, Romanyuk O, Siu C-H. Involvement of Src family kinases in N-cadherin phosphorylation and beta-catenin dissociation during transendothelial migration of melanoma cells. Mol Biol Cell. 2006;17:1261–72.

14. Eustace AJ, Crown J, Clynes M, O'Donovan N. Preclinical evaluation of dasatinib, a potent Src kinase inhibitor, in melanoma cell lines. J Transl Med. 2008;6:53.

15. Oneyama C, Hikita T, Nada S, Okada M. Functional dissection of transformation by c-Src and v-Src. Genes Cells. 2008;13:1–12.

16. Homsi J, Cubitt CL, Zhang S, Munster PN, Yu H, Sullivan DM, et al. Src activation in melanoma and Src inhibitors as therapeutic agents in melanoma. Melanoma Res. 2009;19:167–75.

17. Sánchez-Bailón MP, Calcabrini A, Gómez-Domínguez D, Morte B, Martín-Forero E, Gómez-López G, et al. Src kinases catalytic activity regulates proliferation, migration and invasiveness of MDA-MB-231 breast cancer cells. Cell Signal. 2012;24:1276–86.

18. Andrä K, Lassmann H, Bittner R, Shorny S, Fässler R, Propst F, et al. Targeted inactivation of plectin reveals essential function in maintaining the integrity of skin, muscle, and heart cytoarchitecture. Genes Dev. 1997;11:3143–56.

19. Steinböck FA, Wiche G. Plectin: a cytolinker by design. Biol Chem. 1999;380:151–8.

20. Matsubara T, Yaginuma T, Addison WN, Fujita Y, Watanabe K, Yoshioka I, et al. Plectin stabilizes microtubules during osteoclastic bone resorption by acting as a scaffold for Src and Pyk2. Bone. 2020;132:115209.

21. Bausch D, Thomas S, Mino-Kenudson M, Fernández-del CC, Bauer TW, Williams M, et al. Plectin-1 as a novel biomarker for pancreatic cancer. Clin Cancer Res. 2011;17:302–9.

22. Katada K, Tomonaga T, Satoh M, Matsushita K, Tonoike Y, Kodera Y, et al. Plectin promotes migration and invasion of cancer cells and is a novel prognostic marker for head and neck squamous cell carcinoma. J Proteomics. 2012;75:1803–15.

23. Tamura I, Ueda K, Nishikawa T, Kamada A, Okamura T, Matsuda Y, et al. Expression of Plectin-1 and Trichohyalin in Human Tongue Cancer Cells. OJST. 2018;08:196–204.

24. Meier SM, Kreutz D, Winter L, Klose MHM, Cseh K, Weiss T, et al. An Organoruthenium Anticancer Agent Shows Unexpected Target Selectivity For Plectin. Angew Chem Int Ed Engl. 2017;56:8267–71.

25. Klose MHM, Schöberl A, Heffeter P, Berger W, Hartinger CG, Koellensperger G, et al. Serum-binding properties of isosteric ruthenium and osmium anticancer agents elucidated by SEC-ICP-MS. Monatsh Chem. 2018;149:1719–26.

26. Ogawa M, Yaginuma T, Nakatomi C, Nakajima T, Tada-Shigeyama Y, Addison WN, et al. Transducin-like enhancer of split 3 regulates proliferation of melanoma cells via histone deacetylase activity. Oncotarget. 2019;10:404–14.

27. Matsubara T, Kinbara M, Maeda T, Yoshizawa M, Kokabu S, Takano Yamamoto T. Regulation of osteoclast differentiation and actin ring formation by the cytolinker protein plectin. Biochem Biophys Res Commun. 2017;489:472–6.

28. Matsubara T, Kokabu S, Nakatomi C, Kinbara M, Maeda T, Yoshizawa M, et al. The Actin-Binding Protein PPP1r18 Regulates Maturation, Actin Organization, and Bone Resorption Activity of Osteoclasts.

Mol Cell Biol. 2018;38:e00425-17.

29. Matsubara T, Addison WN, Kokabu S, Neff L, Horne W, Gori F, et al. Characterization of unique functionalities in c-Src domains required for osteoclast podosome belt formation. J Biol Chem. 2021;:100790.

30. Kirihara Y, Takechi M, Kurosaki K, Kobayashi Y, Kurosawa T. Anesthetic effects of a mixture of medetomidine, midazolam and butorphanol in two strains of mice. Exp Anim. 2013;62:173–80.

31. Nakanishi M, Hata K, Nagayama T, Sakurai T, Nishisho T, Wakabayashi H, et al. Acid activation of Trpv1 leads to an up-regulation of calcitonin gene-related peptide expression in dorsal root ganglion neurons via the CaMK-CREB cascade: a potential mechanism of inflammatory pain. Mol Biol Cell. 2010;21:2568–77.

32. Tada Y, Kokabu S, Sugiyama G, Nakatomi C, Aoki K, Fukushima H, et al. The novel IκB kinase β inhibitor IMD-0560 prevents bone invasion by oral squamous cell carcinoma. Oncotarget. 2014;5:12317–30.

33. Liu Y, Qi X, Li G, Sowa G. Caveolin-2 deficiency induces a rapid anti-tumor immune response prior to regression of implanted murine lung carcinoma tumors. Sci Rep. 2019;9:18970.

34. Miyawaki A, Rojasawasthien T, Hitomi S, Aoki Y, Urata M, Inoue A, et al. Oral Administration of Geranylgeraniol Rescues Denervation-induced Muscle Atrophy via Suppression of Atrogin-1. In Vivo. 2020;34:2345–51.

35. Shirakawa T, Miyawaki A, Matsubara T, Okumura N, Okamoto H, Nakai N, et al. Daily Oral Administration of Protease-Treated Royal Jelly Protects Against Denervation-Induced Skeletal Muscle Atrophy. Nutrients. 2020;12.

36. Nath S, Devi GR. Three-dimensional culture systems in cancer research: Focus on tumor spheroid model. Pharmacol Ther. 2016;163:94–108.

37. Talantov D, Mazumder A, Yu JX, Briggs T, Jiang Y, Backus J, et al. Novel genes associated with malignant melanoma but not benign melanocytic lesions. Clin Cancer Res. 2005;11:7234–42.

38. Stover DR, Liebetanz J, Lydon NB. Cdc2-mediated modulation of pp60c-src activity. J Biol Chem. 1994;269:26885–9.

39. Resnick RJ, Taylor SJ, Lin Q, Shalloway D. Phosphorylation of the Src substrate Sam68 by Cdc2 during mitosis. Oncogene. 1997;15:1247–53.

40. Matsuyoshi N, Hamaguchi M, Taniguchi S, Nagafuchi A, Tsukita S, Takeichi M. Cadherin-mediated cell-cell adhesion is perturbed by v-src tyrosine phosphorylation in metastatic fibroblasts. J Cell Biol. 1992;118:703–14.

41. Rötzer V, Hartlieb E, Vielmuth F, Gliem M, Spindler V, Waschke J. E-cadherin and Src associate with extradesmosomal Dsg3 and modulate desmosome assembly and adhesion. Cell Mol Life Sci. 2015;72:4885–97.

42. Bruzzaniti A, Neff L, Sanjay A, Horne WC, De Camilli P, Baron R. Dynamin forms a Src kinase-sensitive complex with Cbl and regulates podosomes and osteoclast activity. Mol Biol Cell. 2005;16:3301–13.

43. Ory S, Brazier H, Pawlak G, Blangy A. Rho GTPases in osteoclasts: orchestrators of podosome arrangement. Eur J Cell Biol. 2008;87:469–77.

44. Guarino M. Src signaling in cancer invasion. J Cell Physiol. 2010;223:14–26.

45. Boczonadi V, McInroy L, Määttä A. Cytolinker cross-talk: periplakin N-terminus interacts with plectin to regulate keratin organisation and epithelial migration. Exp Cell Res. 2007;313:3579–91.

46. Winter L, Wiche G. The many faces of plectin and plectinopathies: pathology and mechanisms. Acta Neuropathol. 2013;125:77–93.

47. Moch M, Windoffer R, Schwarz N, Pohl R, Omenzetter A, Schnakenberg U, et al. Effects of plectin depletion on keratin network dynamics and organization. PLoS One. 2016;11:e0149106.

48. Gache Y, Chavanas S, Lacour JP, Wiche G, Owaribe K, Meneguzzi G, et al. Defective expression of plectin/HD1 in epidermolysis bullosa simplex with muscular dystrophy. J Clin Invest. 1996;97:2289–98.

49. Shimizu H, Masunaga T, Kurihara Y, Owaribe K, Wiche G, Pulkkinen L, et al. Expression of plectin and HD1 epitopes in patients with epidermolysis bullosa simplex associated with muscular dystrophy. Arch Derm Res. 1999;291:531–7.

50. Destaing O, Block MR, Planus E, Albiges-Rizo C. Invadosome regulation by adhesion signaling. Curr Opin Cell Biol. 2011;23:597–606.

51. Sutoh Yoneyama M, Hatakeyama S, Habuchi T, Inoue T, Nakamura T, Funyu T, et al. Vimentin intermediate filament and plectin provide a scaffold for invadopodia, facilitating cancer cell invasion and extravasation for metastasis. Eur J Cell Biol. 2014;93:157–69.

Figures

Figure 1

Src signaling is impaired in plectin deficient cells.

(A) Plectin levels in control B16 and 2 clones of plectin deficient B16 cells (PKO1 and PKO2) were determined by western blotting analysis. Full uncropped blots are shown in Fig S6. (B) Expression and phosphorylation of Pyk2, or GapDH was determined by western blotting assay 24 h after plating. Full uncropped blots are shown in Fig S6. (C) Src was immunoprecipitated (IP:Src) with an anti-Src antibody and interaction with Pyk2 was detected by western blotting analysis. Full uncropped blots are shown in Fig S7. (D) Cells were stained with Rhodamine-phalloidin. Long actin fiber is shown by arrow. Scale bar = 25 μm.

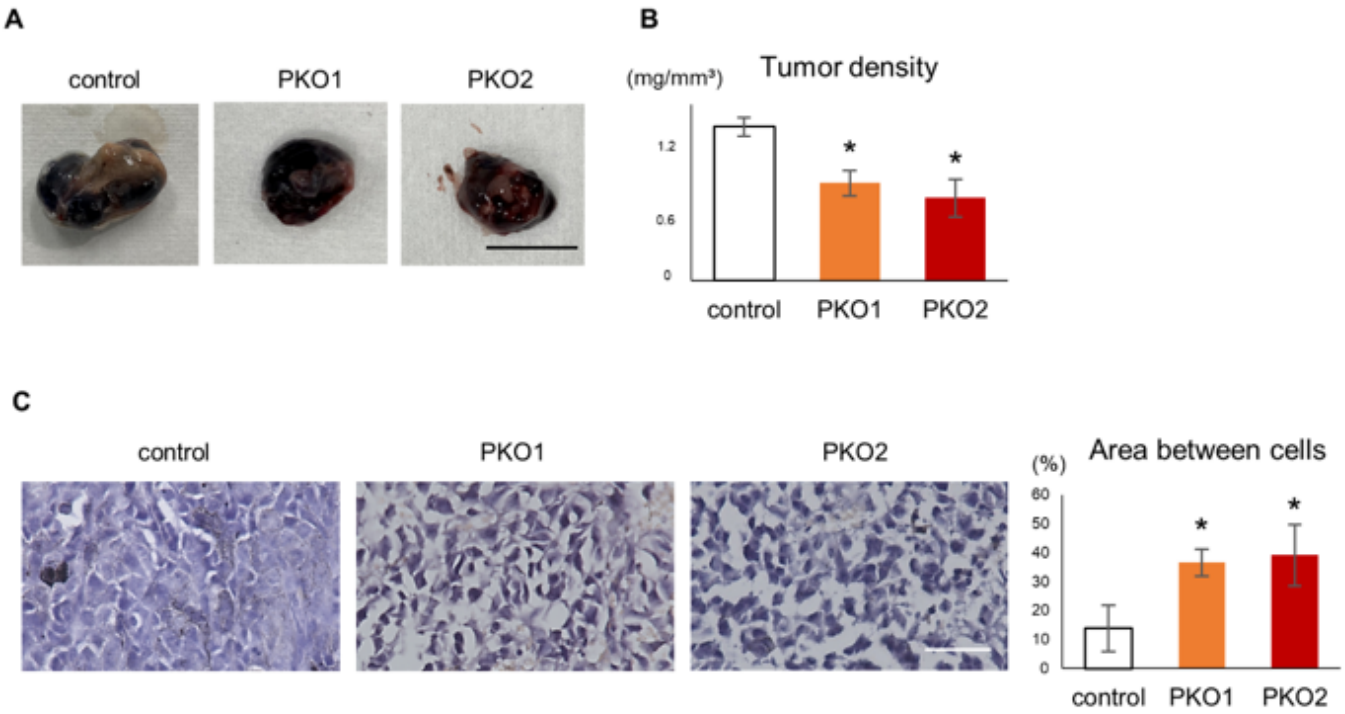

Figure 2

Plectin knockout cells form sparse tumors.

(A) Control or PKO cells (1×10^5 cells per mouse) were subcutaneously injected into BALB/cAJcl-nu/nu mice (n = 8). Photographs of extracted tumors 2 weeks after injection. Scale bar = 10 mm. (B) Tumor density was calculated from excised tumor weight and volume. Averages of the total tumor density of all tumors excised from each mouse is shown in the graph. (*; $p < 0.05$ vs control). (C) Sections of tumors were stained with H&E. Scale bar = 50 μm. The area between cells was measured and calculated by ImageJ (*; $p < 0.05$ vs control).

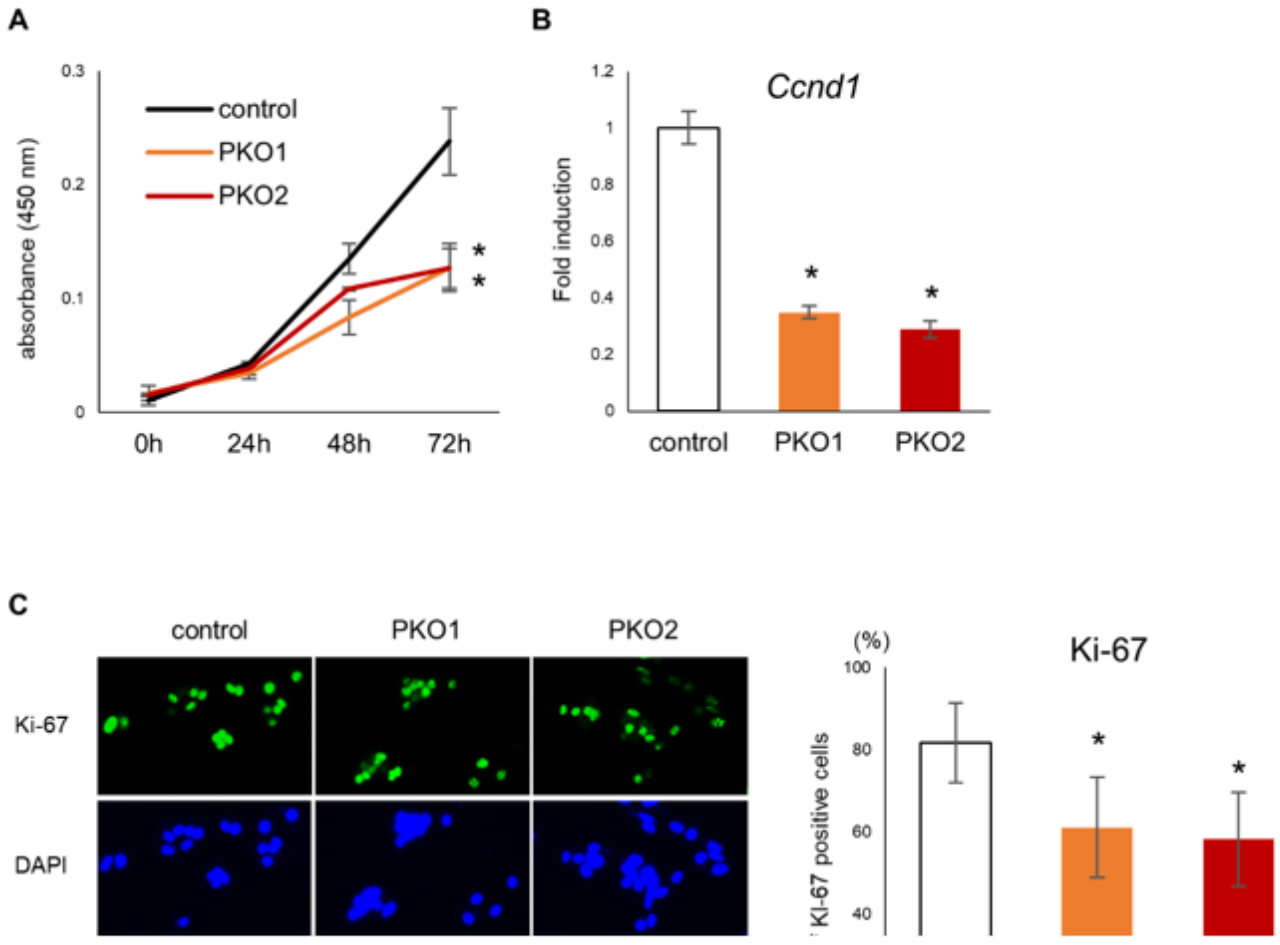

Figure 3

Cell proliferation is decreased in plectin knockout cells.

(A) Cells were plated at a density of 5×10³ cells per well in 96 well plate and the number of viable cells measured by WST-8 assay at the indicated time (n = 4, *; $p < 0.05$ vs control). (B) mRNA was harvested from control or PKO cells 1 d after plating. Expression of *Ccnd1* was determined by real time qPCR (n = 3, *; $p < 0.05$ vs control). (C) Cells were fixed and stained with anti-Ki-67/Alexa fluor 488 and DAPI at 1 d after plating. The ratio of Ki-67 positive cells vs DAPI positive cells was calculated and indicated to graph at right side. Scale bar = 50 μm. (n = 5, *; $p < 0.05$ vs control).

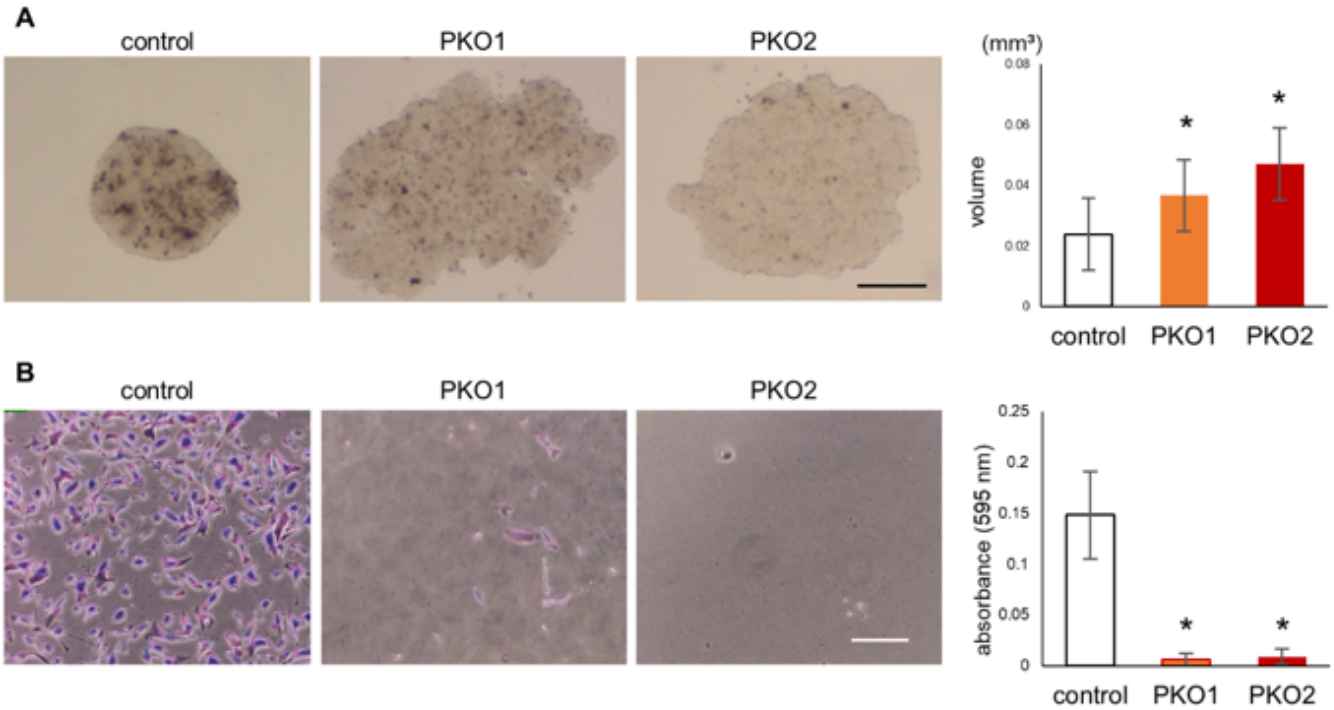

Figure 4

Cell adhesion is impaired in plectin knockout cells.

(A) Cells were cultured at a density of 5×10³ cells per 15 µl drop on the inner side of a dish lid to form spheroids for 7d. They were observed by stereoscopic microscope and measured the sizes by ImageJ. Scale bar = 250 µm (n = 5, *; P< 0.05 vs control). (B) Cells were plated on a fibronectin-coated dish and counted the number of adherent cells after 2 h. The adherent cells were stained with crystal violet (left 3 panels). After taken photo, the adherent cells were lysed and measured the absorbance shown at graph (right panel) (n = 6, *; p < 0.05 vs control).

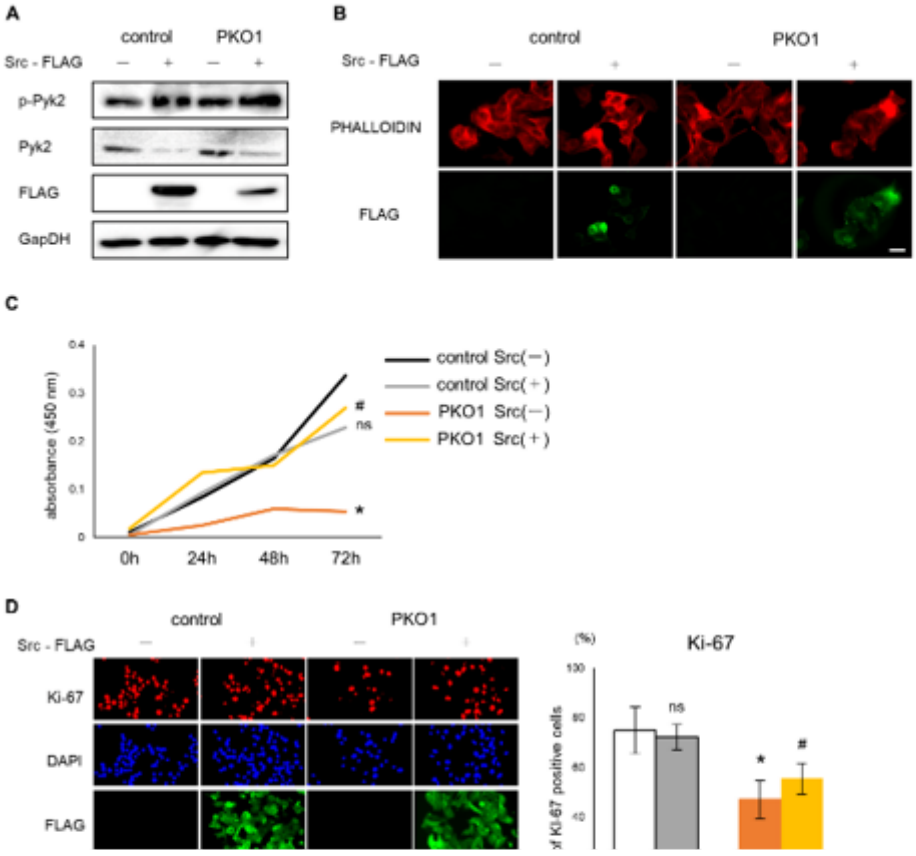

Figure 5

Src overexpression rescues cell proliferation and adhesion of plectin knockout melanoma cells.

(A) Src was overexpressed in B16 and PKO1. Expression and phosphorylation of Pyk2 was determined by western blotting analysis. Full uncropped blots are shown in Fig S9. (B) Cells were plated at 1 d after Src introduction. The number of viable cells was determined by WST-8 assay at indicated time (n = 3, *; $p < 0.05$ vs control group, #; $p < 0.05$ vs PKO group). (C) Cells were fixed and stained with DAPI, anti-Ki-67/Alexa fluor 555 and anti-FLAG/Alexa fluor 488 at 1 d after plating. The ratio of Ki-67 positive cells vs DAPI positive cells was calculated and shown at graph. Scale bur = 100 μm (n = 5, *; $p< 0.05$ vs control group, #; $p < 0.05$ vs PKO group). (D) Src was introduced into the cells for 1 d. Cells were cultured at

5×10³ cells per 15 µl drop on a dish lid to form spheroid for 7 d. Spheroids were observed by stereoscopic microscope and measured by ImageJ. Scale bar = 500 µm (n = 6, *; $p < 0.05$ vs control group, #; $p < 0.05$ vs PKO group). (E) Cells were plated on a fibronectin-coated dish 1 d after Src introduction. After 2 h incubation, the adherent cells were stained with crystal violet (left 6 panels) and counted (right panel). Scale bar = 10 µm (n = 6, *; $p < 0.05$ vs control group, #; $p < 0.05$ vs PKO group). (F) Cells were immunostained with anti-FLAG/Alexa fluor 488, Rhodamine-phalloidin and DAPI at 2 d after Src introduction. Scale bar = 50 µm. (n = 6, *; $p < 0.05$ vs control group, #; $p < 0.05$ vs PKO group).

Supplementary Files

This is a list of supplementary files associated with this preprint. Click to download.

- figures4sup3.pdf